Ordering effects on optical transitions in $Ga_xIn_{1-x}P/(Al_{0.66}Ga_{0.34})_yIn_{1-y}P$ quantum wells studied by photoluminescence and reflectivity spectroscopy

Jun Shao*
4. Physikalisches Institut, Universität Stuttgart, D-70550 Stuttgart, Germany
and National Lab for Infrared Physics, Shanghai Institute of Technical Physics, Chinese Academy of Sciences, 200083 Shanghai, China

Rolf Winterhoff, Achim Dörnen, and Enno Baars
4. Physikalisches Institut, Universität Stuttgart, D-70550 Stuttgart, Germany

Junhao Chu
National Lab for Infrared Physics, Shanghai Institute of Technical Physics, Chinese Academy of Sciences, 200083 Shanghai, China
(Received 2 July 2003; published 20 October 2003)

Optical transitions are investigated systematically by excitation-density dependent photoluminescence (PL), magneto-PL, and reflectivity spectroscopies in ordered $Ga_xIn_{1-x}P/(Al_{0.66}Ga_{0.34})_yIn_{1-y}P$ quantum-well (QW) structures with different strain, substrate orientation, and capping layer. Blueshift and narrowing of the PL peak are observed as the excitation density increases in the range of $\lesssim 40$ W/cm^2 and approach nearly constant values as the excitation gets higher. They are affected by strain, substrate and doping of the capping layer. A larger blueshift corresponds to a larger stable line width of the PL peak measured at a high excitation level. In the magneto-PL measurements, the excitonic feature of the PL transition is clearly identified. The Stokes shift of the first peak in the reflectivity spectrum relative to the corresponding PL peak is also affected by strain, substrate misorientation, and doping of the capping layer. With the observations, (i) the assumptions are checked to be unreasonable of the spatially type-II band alignment and the band-tail states in the case of QW's. (ii) The existence of domain distribution and order-induced piezoelectric field is verified and the scattering of the domain distribution ($\Delta\eta$) and the magnitude of the piezoelectric field ($e_{\mathrm{pe},\perp}$) are estimated. (iii) The $\Delta\eta$ is obviously larger in the QW's than that determined previously in $GaInP_2$ bulk alloy. It takes a large value for the sample with (001) GaAs substrate and a small value for that with 6° off toward $[111]_B$ misaligned (001) GaAs substrate. (iv) The $e_{\mathrm{pe},\perp}$ is significantly smaller in the QW's than the theoretical prediction for the $GaInP_2$ bulk alloy. It is relatively high for the sample with the (001) GaAs substrate, and is obviously enhanced by the Zn-doped GaP capping layer. The results clarify that the optical transitions can be well interpreted with the combination of the $\Delta\eta$ and $e_{\mathrm{pe},\perp}$ in the QW's. A model is hence established in understanding the optical phenomena based on the concepts of the domain distribution and the piezoelectric field.

DOI: 10.1103/PhysRevB.68.165327 PACS number(s): 78.67.De, 78.30.Fs, 78.55.Cr, 78.20.Ls

I. INTRODUCTION

Under proper growth conditions, epitaxially grown $Ga_xIn_{1-x}P$ alloy exhibits CuPt-type ordering along the $[111]_B$ directions.[1] The local ordering parameter η ($0 \leqslant \eta \leqslant 1$) is substrate-misorientation dependent. It was suggested that domains characterized by a distribution function $F(\eta)$ may be formed in $GaInP_2$ bulk material.[2] Supports of the domain distribution have been established in spatially resolved photoluminescence (PL) studies.[3–5] The ordering causes prominent changes to the electronic band structures and optical properties of the $Ga_xIn_{1-x}P$ alloy. In the last several years, extensive theoretical and experimental studies have been conducted in investigating ordering-induced band-gap reduction and valence-band splitting,[6–13] anisotropy of the optical transitions,[14–16] and polarization electric fields and their effects on band offsets.[17–19]

Low temperature PL studies[20,21] illustrated that the PL spectra from ordered $GaInP_2$ bulk alloy could be classified in three types, of which a distinct feature was the coexistence of a nonexcitonic ''moving peak'' at a lower energy with an excitonic peak at a higher energy. The energetic separation between the two peaks was correlated to the ordering. It was peculiar that while the moving peak showing energetic blue shift the excitonic peak manifests no shift upon increasing excitation power density. To address the origin of the moving peak, assumptions were proposed of spatially indirect recombination occurring at domain boundaries of different degree of ordering[3,21–24] and band-tail states due to, e.g., shallow traps.[21]

Recently, two new models were employed in explaining the ordering dependence of carrier lifetimes in ordered $Ga_{0.52}In_{0.48}P/GaAs$,[25] in light of the progress in theoretical studies.[26,27] One of the models was based on the plane-wave pseudopotential calculations of Mattila *et al.* that (111) layer thickness fluctuations (sequence mutations) may occur in the form of In-In double layers embedded in the CuPt-ordered $GaInP_2$ matrix, during the growth of $GaInP_2$ alloy.[26] Such sequence mutations induce localized hole states energetically above the CuPt-confined hole states. As the lowest conduction band is confined in the CuPt region, the transition to the localized hole states is spatially indirect. The other one originated from the first-principle pseudopotential calculations of Froyen *et al.* that the ordered/disordered $GaInP_2$ interface

TABLE I. Samples parameters and experimental data of the ordered $Ga_xIn_{1-x}P/(Al_{0.66}Ga_{0.34})_yIn_{1-y}P$ QW's established by PL and optical reflectivity measurements. The ordering parameter η was determined with the procedure discussed in Ref. 34. Except for T, x, η, and $\Delta\eta$, the parameters $e_{pe,\perp}$ and $\eta^2 e_{pe,\perp}$ are in the unit of kV/cm, others are in the unit of meV. Undop stands for 2-nm-thick undoped GaInP capping layer, and Zn-dop for 410-nm-thick Zn-doped GaP capping layer.

Sample		I			II			III		IV
	6°*A*	0°	6°*B*	6°*A*	0°	6°*B*	0°	6°*B*	0°	6°*B*
T(°C)	700	700	700	700	700	700	700	700	750	750
Capping	undop	undop	undop	Zn-dop	Zn-dop	Zn-dop	undop	undop	Zn-dop	Zn-dop
x	0.52	0.52	0.52	0.52	0.52	0.52	0.40	0.40	0.40	0.40
η	0.21	0.40	0.50	0.22	0.34	0.44	0.30	0.33	0.29	
Blueshift	0.2	5.0	3.4	0.7	7.1	1.5	10.5	2.3	6.3	2.3
Narrowing	−1.5	1.9	1.4	1.9	3.3	3.2	1.0	1.3	2.1	1.3
PL LW_s	11.2	18.6	12.2	16.5	23.2	15.3	27.1	20.0	23.4	29.8
Stokes shift	7.0	20.3	18.7	−1.1	35.7	22.1	16.2	10.3	27.4	
LW_{DR}	12.0	17.1	14.7	10.5	30.9	13.0	16.4	15.5	15.6	
$\Delta\eta$	0.07	0.08	0.05	0.03	0.20	0.04	0.13	0.11	0.13	
$e_{pe,\perp}$		106	48	331	216	103	167	129	238	
$\eta^2 e_{pe,\perp}$		17	12	16	25	20	15	14	20	18

has type-I band alignment, and the ordered region has a strong macroscopic electric polarization.[27] The polarization generates a strong internal electric field in ordered $GaInP_2$, by which the experimental phenomena can be interpreted without a type-II band alignment. Note, however, that the question of the magnitude of this electric field is still open, and hence awaiting new experiments.[18]

The fact that by including ordering one could alter the materials properties of an alloy without changing its chemical composition opened novel technological opportunities. In $Ga_xIn_{1-x}P$/AlGaInP QW systems, it was illustrated that the ordering could be used to optimize optoelectronic devices or even to develop new device concepts.[28,29] In contrast to the bulk material, however, few studies were available concerning ordering effects on, e.g., optical transitions[30,31] and band-edge electronic structures[32–34] in the QW systems.

In this work, PL and reflectivity measurements are performed on ordered $Ga_xIn_{1-x}P/(Al_{0.66}Ga_{0.34})_yIn_{1-y}P$ QW samples. Two types of PL line profiles are identified, one of which is single peak and the other is slightly separated double peak. For the single-peak samples, distinct phenomena are observed simultaneously of blueshift and narrowing as the excitation-power density increases. The blueshift and narrowing approach nearly constant values at an excitation density of $\gtrsim 40$ W/cm^2. Excitonic feature of the PL peak is evidenced by magneto-PL measurements. A model is proposed based on the concepts of domain distribution and order-induced piezoelectric field, and is illustrated to be applicable in explaining the experimental phenomena. The magnitudes of the scattering of the domain distribution and the piezoelectric field are also estimated, and manifest dependence on strain, substrate misorientation, and doping of the capping layer.

II. EXPERIMENT

Four series $Ga_xIn_{1-x}P/(Al_{0.66}Ga_{0.34})_yIn_{1-y}P$ QW samples are studied in this work, each consists of three samples. They were grown on (001) Si-doped GaAs substrate by metal-organic vapor-phase epitaxy with a similar structure but different substrate misorientation, i.e., 0°, 6° off toward $[111]_A$ (denoted as 6°*A* hereafter), 6° off toward $[111]_B$ (denoted as 6°*B*), respectively. On top of the substrate, a 30-nm-thick GaAs buffer layer was grown, followed by a 2-nm-thick GaInP layer and a 20-nm-thick $(Al_{0.66}Ga_{0.34})_{0.52}In_{0.48}P$ layer. Then ten periods of 10-nm-$Ga_xIn_{1-x}P$/4-nm-$(Al_{0.66}Ga_{0.34})_yIn_{1-y}P$ QW's were grown, with a 50-nm-thick $(Al_{0.66}Ga_{0.34})_{0.52}In_{0.48}P$ buffer layer and a capping layer as the end of the structure. Two strain conditions were realized of compressive strain with a combination of $x=0.40$ and $y=0.76$ for the series III and IV samples and unstrain (lattice match) with $x\simeq 0.52$ and $y=0.52$ for the series I and II samples. The series I and III samples have a 2-nm-thick GaInP capping layer, whereas the series II and IV have a 410-nm-thick Zn-doped GaP capping layer. The series IV samples were prepared at a temperature of 750 °C. The other three series samples were prepared at a temperature of 700 °C. The details of the samples parameters are summarized in Table I, together with the experimental data established in the following sections.

The samples were arranged in the center of a superconducting split-coil magnet in a Zeeman cryostat and were kept at a temperature around 1.8 K. The Faraday configuration of the magnet was used. The magnetic field was adjustable continuously in the range of 0 − 6.8 T. To record optical spectra, a Fourier-transformed-infrared spectrometer was employed. In the PL measurements, an Ar^+-ion laser acted as exciting source with its wavelength being set at 514.5 nm. Light from the laser first went through a laser-power controller so as to keep the output power stable and to drastically reduce laser noise. A visible beam-splitter and a liquid-nitrogen cooled Ge detector were used. In the reflectivity measurements, a conventional halogen-lamp served as excitation source and a Si-diode detector were used. A spectral range of

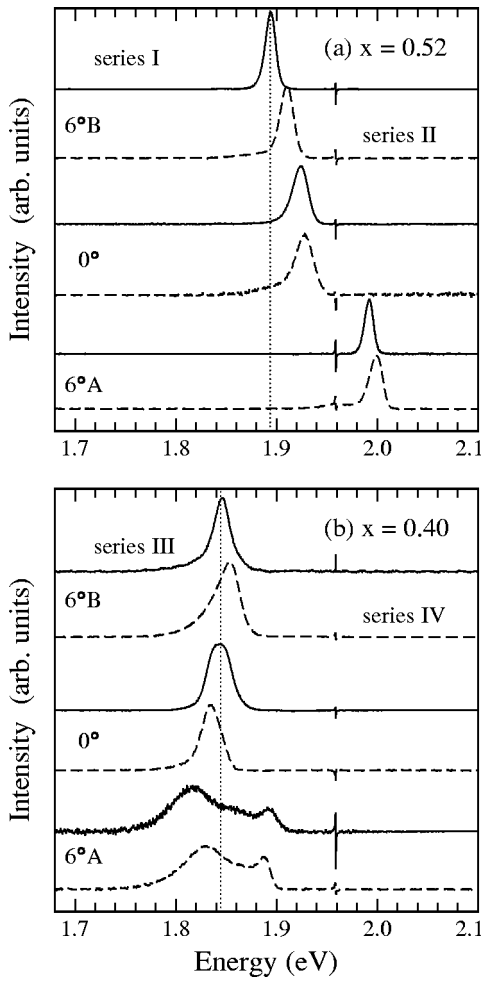

FIG. 1. PL spectra from (a) lattice matched ($x=0.52$,$y=0.52$) and (b) compressively strained ($x=0.40$,$y=0.76$) $Ga_xIn_{1-x}P/(Al_{0.66}Ga_{0.34})_yIn_{1-y}P$ QWs with different substrate misorientations. Dashed lines represent series II and IV and solid lines represent series I and III samples, respectively, in (a) and (b). Vertical dotted lines correspond to the energies of the series I and III samples with the $6°B$ substrate, respectively.

11 500–18 000 cm^{-1} was warranted at a resolution of 6 cm^{-1} ($\sim$0.7 meV).

III. RESULTS

Figure 1 illustrates the typical PL spectra from the lattice matched (a) and compressively strained (b) $Ga_xIn_{1-x}P/(Al_{0.66}Ga_{0.34})_yIn_{1-y}P$ QW's with different substrate misorientations. The dashed lines are for the series II and IV, and the solid lines for the series I and III samples, respectively. The sparks occurring in all the PL spectra at $\sim$1.96 eV are introduced by the He-Ne laser of the FTIR spectrometer. Unlike the classification of three types of PL-line profiles in ordered $GaInP_2$ bulk material,[21] here only two types are identified: (i) One has a single peak and is for all the lattice-matched samples and the compressively strained ones with the 0° and $6°B$ substrates and the other (ii) shows slightly separated double peaks and is for the $6°A$ compressively strained samples.

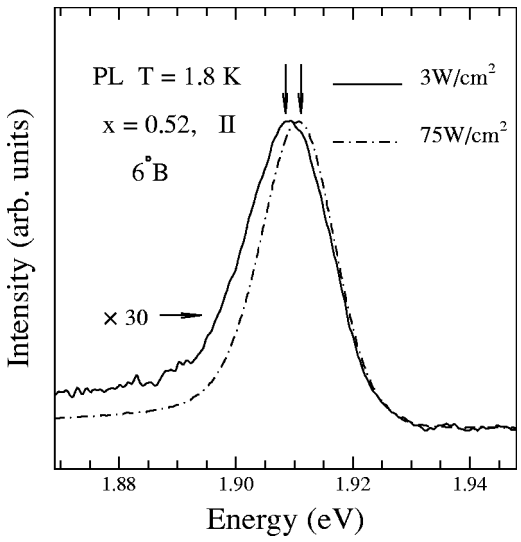

FIG. 2. PL spectra recorded at different excitation densities for the series II lattice-matched sample with the $6°B$ substrate. The intensity of the spectrum at lower excitation is multiplied by 30 to match the other spectrum. The downward arrows indicate the peak energies of the two spectra, respectively.

For the lattice-matched samples shown in Fig. 1(a), the PL peaks occur at highest energies for the $6°A$ substrate and at lowest energies for the $6°B$ substrate. This is consistent with the established knowledge.[16] For the compressively strained samples shown in Fig. 1(b), however, two exceptions exist that the series IV sample with the $6°B$ substrate has significantly higher transition energy than that with the 0° substrate, and the ''low-energy'' peak of the samples with the $6°A$ substrate even occurs at the lowest energy position in the same series.

Due to the lattice mismatch between the thick Zn-doped GaP capping layer and its adjacent barrier/QW layers, an additional compressive strain may be introduced in the series II and IV samples. This will reduce the PL transition energy with respect to the counterpart with a GaInP capping layer. From the PL spectra, it can be seen, however, the effect should be significantly weaker than that introduced by changing Ga composition from 0.52 to 0.40 in the QW's. For the compressively strained samples, the difference in the transition energy is very small for the two series samples with an identical substrate. For the lattice-matched samples, on the other hand, the samples with the GaP capping layer has slightly higher transition energy for each particular substrate.

A. Excitation-density dependent photoluminescence

Figure 2 depicts two spectra recorded at different excitation densities for the series II sample with the $6°B$ substrate. The intensity of the spectrum at lower excitation is multiplied by a factor of 30 to match the other spectrum at higher excitation level. The blueshift as well as narrowing of the PL peak is clearly identified as the excitation density increases.

In Fig. 3, typical tendency of the peak energy is shown as a function of the excitation density. For the single-peak

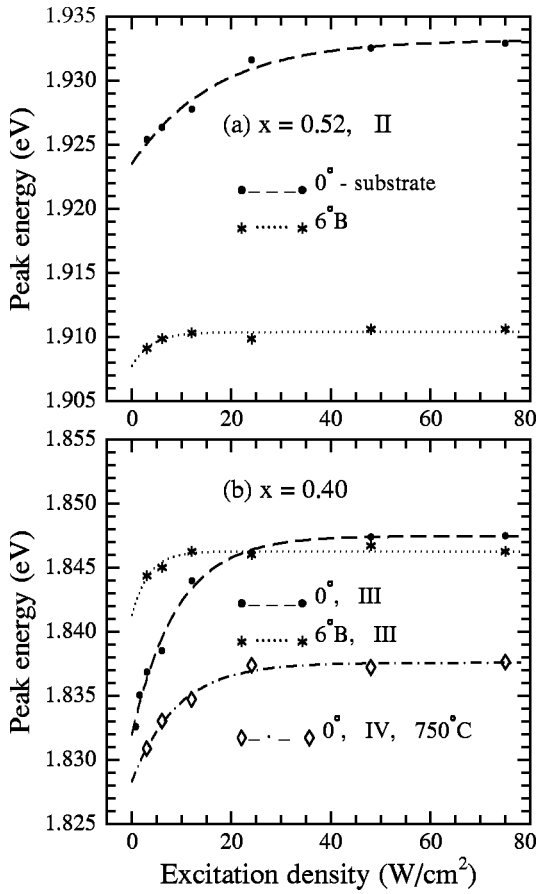

FIG. 3. Excitation-density dependence of the PL transition energies for (a) the series II ($x=0.52$) $Ga_xIn_{1-x}P/(Al_{0.66}Ga_{0.34})_{0.52}In_{0.48}P$ QW samples with the 0° and 6°*B* substrates (denoted by ●- -● and *···*, respectively), and (b) the series III ($x=0.40$) QW samples with the 0° and 6°*B* substrates (denoted by ●- -● and *···*, respectively) and the series IV sample with the 0° substrate (denoted by ◇- · -◇), respectively. Lines are fitted to the measuring points as a guide to the eyes.

samples, the PL peak shifts first rapidly to higher energies with increasing the excitation density in the range below 15 W/cm^2, then slowly, and finally does not show any significant increase further in the range $\gtrsim$40 W/cm^2. This was not the case for the measurement on $GaInP_2$ bulk material,[21] whereby the blueshift was identified for the moving peak to be strong in a range of the excitation density up to 500 W/cm^2. The reason will be discussed in Sec. IV. It is noteworthy that the degree of the ''saturation'' of the blueshift depends on the substrate misorientation: while the samples with the 0° substrate still manifest slight blueshift with the excitation density, those with the 6°*B* substrate do not show blueshift further. Also observed is that the magnitude of the blueshift varies with substrate misorientation. The lattice-matched sample with the 0° substrate [denoted by ●- -● in Fig. 3(a)] shows a blueshift of about 7 meV, while the 6°*B* substrate (denoted by *···*) only a value of 1.5 meV and the 6°*A* substrate below 0.7 meV, in the range of the excitation density being employed. Similar tendency but enlarged value of the blueshift is observed for the series III (compressively strained) samples with the 0° and 6°*B* substrates as illustrated in Fig. 3(b). The sample's growth temperature and/or the doping of the capping layer also affect the blueshift. As can be seen in Fig. 3(b), the blueshift of the sample prepared at 700 °C with the 0° substrate (denoted by ●- -●) is nearly two times as large as that of the counterpart prepared at 750 °C with Zn-doped GaP capping layer (denoted by ◇-·-◇).

Concerning the PL peak line width [full-width at half-maximum (FWHM)], it first decreases ($\sim$0.5$-$1.5 meV) as the excitation density increases up to $\sim$15 W/cm^2, then keeps nearly constant for higher excitation density for most of the single-peak samples. An exception is that the lattice-matched sample with the 6°*A* substrate and Zn-doped capping layer manifests further peak narrowing as the excitation density gets higher. This will be discussed in Sec. IV.

The change in the FWHM is also strain- and substrate-misorientation dependent. As shown in Fig. 4, the lattice-matched samples manifest more significant PL-peak narrowing than the corresponding compressively strained ones. And the lattice-matched samples with the 0° and 6°*B* substrates correspond to a sharper peak narrowing than the sample with the 6°*A* substrate. Even more, the series I sample with the 6°*A* substrate shows a slight increase to the peak width of $\sim$1.5 meV (not illustrated in Fig. 4), its corresponding blueshift, however, is nearly undetectable ($\leqslant$0.2 meV) as the excitation-density increases. Similar comparison for the compressively strained samples is difficult, as the sample with the 6°*A* substrate corresponds to a slightly separated double peak for which the FWHM is difficult to exactly determine. It is worthy to mention that unlike the blueshift, the narrowing of the PL peak is more obvious for the series IV sample prepared at 750 °C with a Zn-doped GaP capping layer than for the corresponding series III sample prepared at 700 °C without a doped capping layer.

The values of the PL-peak blueshift, narrowing, and stable linewidth are summarized in Table I for all four series samples. The results illustrate a general relation between the blueshift and the stable linewidth (LW_s) of the PL peak measured at high excitation density ($\sim$50 W/cm^2): a larger blueshift corresponds to a larger stable FWHM. The 6°*B* lattice-matched samples have relatively small FWHM, 12.2–15.3 meV, similar to the 6°*A* samples. In contrast, the 0° samples have a large value 18.6–23.2 meV. Similar but enlarged values (20.0 meV for the 6°*B* and 27.1 meV for the 0° sample) are observed for the series-III compressively strained samples. For the series-IV samples prepared at 750 °C with a Zn-doped GaP capping layer, however, the 0° sample has a smaller FWHM (23.4 meV) than the counterpart of the series III sample prepared at 700° without a doped capping layer, and the value is even smaller than the 6°*B* sample (29.8 meV) in the same series. It is worthy to emphasize that the line shape of the 6°*B* sample of series IV is obviously asymmetric with its maximum occurring at higher energy than the 0° sample, suggesting a bad sample quality. Further evidence is revealed shortly afterward by magneto-PL and reflectivity measurements.

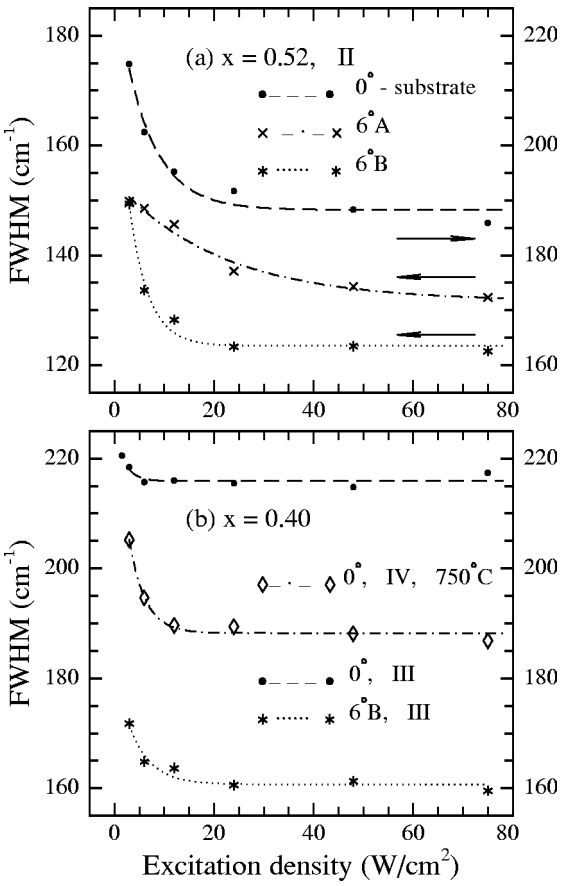

FIG. 4. Full-width at half-maximum (FWHM) of the PL peak determined by curve-fitting procedure plotted against the excitation density for (a) the series II lattice-matched $Ga_xIn_{1-x}P/(Al_{0.66}Ga_{0.34})_{0.52}In_{0.48}P$ QW samples with the 0° (denoted by ●- -●), 6°*A* (denoted by ×-·-×) and 6°*B* (denoted by *···*) substrates, respectively and (b) the series III compressively strained QW samples with the 0° (denoted by ●- -●) and 6°*B* (denoted by *···*) substrates, and the series-IV compressively strained sample with the 0° substrate (denoted by ◇- · -◇), respectively. The lines are fitted to the corresponding measuring points to guide the eyes. The horizontal arrows in (a) indicate the corresponding data being plotted against the pointed vertical axes.

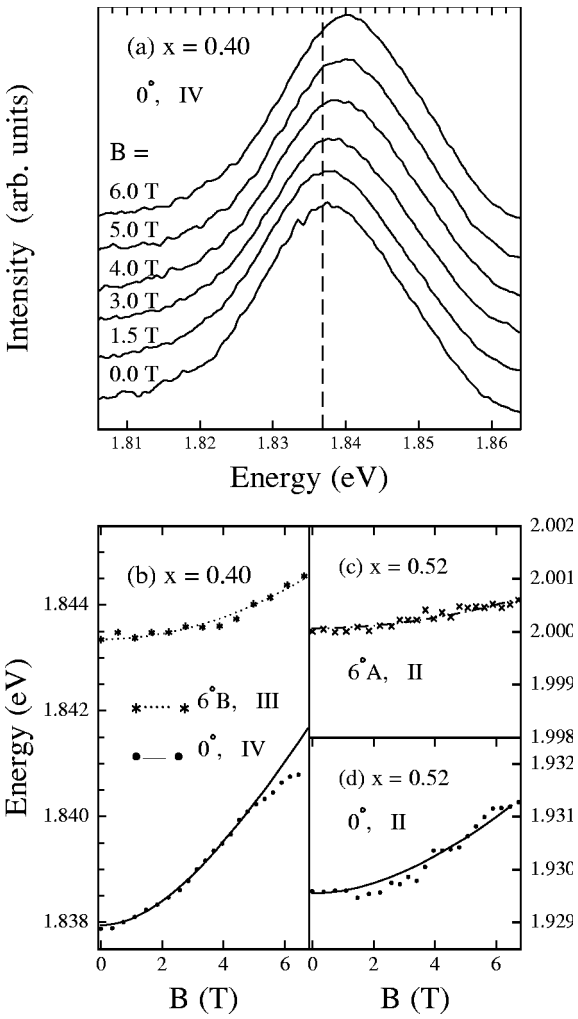

FIG. 5. (a) PL spectra recorded at different magnetic fields for the series IV compressively strained $Ga_{0.4}In_{0.6}P/(Al_{0.66}Ga_{0.34})_{0.76}In_{0.24}P$ QW sample with the 0° substrate. The peak energies are plotted against the magnetic fields for (b) this sample (denoted by ●- -●) and the series III compressively strained sample (denoted by * ··· *) with the 6°*B* substrate, and the series II lattice-matched samples with (c) 6°*A* and (d) 0° substrates. The dashed vertical line in (a) is a guide to the eyes, and the curves in (b)–(d) are theoretical fits to the peak energies based on an effective-mass equation of an exciton in external magnetic fields.

B. Magnetophotoluminescence

Figure 5(a) shows a set of the PL spectra recorded at different magnetic fields for the series IV compressively strained sample with the 0° substrate. The peak energies of the PL spectra are depicted against the magnetic fields for this sample and the 6°*B* series III sample in Fig. 5(b), and for the 6°*A* and 0° series II lattice-matched samples in Figs. 5(c) and 5(d), respectively. Obviously, the PL transition peak shifts to higher energies as the magnetic field *B* increases.

The diamagnetic shift of the 0° compressively strained sample is more significant than the 6°*B* sample. Furthermore, similar diamagnetic shifts have been detected for the 0° and 6°*B* compressively strained samples under high excitation density of $\sim 45-60$ W/cm^2 as well as a low excitation density of ~ 1.5 W/cm^2. It is safely concluded that the PL transitions have a similar origin and correlate with the band-to-band involved transition of the QW's in all the employed excitation levels.

For the series-II lattice-matched sample with the 6°*A* substrate illustrated in Fig. 5(c), very small diamagnetic shift ~ 0.7 meV is observed. In this particular case, the ordering is in a very low degree,[34] $\eta \simeq 0.22$, as listed in Table I, and the highest two valence subbands of the QW's, namely, heavy-hole- (HH-) and light-hole- (LH-) like subbands,[35] are very close to each other as predicted by an ordering-included six-band $\mathbf{k}\cdot\mathbf{p}$ model.[36] The strong interaction between the two subbands results in the diamagnetic shift negligible under medium magnetic fields. For the series II sample with the 0° substrate illustrated in Fig. 5(d), the degree of ordering gets

higher, leading to an additional separation to the two highest valence subbands. The interaction between the subbands is reduced, and hence, a larger diamagnetic shift is detected.

To theoretically simulate the diamagnetic shifts, the effective-mass equation of an exciton in an external magnetic field is employed[37]

$$\left\{-\frac{\hbar^2}{2\mu}\left[\frac{1}{\rho}\frac{\partial}{\partial\rho}\left(\rho\frac{\partial}{\partial\rho}\right)\right]+\frac{e^2}{8\mu}B^2\rho^2+V(\rho)\right\}R_n(\rho) = E_nR_n(\rho), \tag{1}$$

$$V(\rho)=\frac{-e^2}{4\pi\varepsilon_0}\int\int_{-\infty}^{+\infty}\frac{|Z_e(z_e)|^2|Z_h(z_h)|^2}{\varepsilon_r(z_e,z_h)\sqrt{\rho^2+(z_e-z_h)^2}}\,dz_e dz_h, \tag{2}$$

where ρ is the in-well-plane separation between the electron and hole constituting an exciton. μ is exciton reduced effective mass. $Z_e(z_e)$ and $Z_h(z_h)$ are the confined-state wave functions of electrons and holes, respectively. $\varepsilon_r\varepsilon_0$ is the dielectric constant of the well or the barrier depending on z_e and z_h. n represents the nth excitonic state. $R_n(\rho)$ is for the S-type excitonic envelope function. In the calculation, μ is assigned an initial value and is adjusted for each particular sample to achieve a good fit. The results are depicted by the solid and dotted lines in Figs. 5(b)–5(d). As that the theory describes the experimental data quite well, it serves as direct evidence indicating that the PL transition from the QW is excitonic.

It is worthy to mention that a ''negative'' shift is observed with large scattering in the magnetic field range of $0-6$ T for the series IV compressively strained sample with the $6°B$ substrate. This indicates that the PL from the sample is nonexcitonic, and hence provides a direct support to the bad sample-quality assumption in Sec. III A.

C. Optical reflectivity

Figure 6(a) shows reflectivity and PL spectra for the series IV sample with the 0° substrate. As is known, optical reflectivity shows sharp features at the energies of the exciton associated with conduction and valence confinement subband.[38–40] However, the typical reflectivity spectrum is here broad, ''mountainlike'' with apparent extrema located at about 1.82 eV and 2.08 eV, respectively. Such broad features are ascribed to the Fabry-Pérot interference and are determined by the sample thickness.[36] In addition, there are weak fluctuations around 1.86 eV, as marked with three downward arrows. They are due to the transitions in the QW's. To clarify them, a second-order derivative operation is performed on the reflectivity spectrum.[34,37] The second-order derivative of the reflectivity (SODR) is also depicted. Clearly, the SODR manifests clear peaks and dips in the region of about 1.86 eV. All the three peaks in the SODR were shown to originate from the excitonic transitions in the QW layer,[31] and the first two were identified to be HH- and LH-like exciton transitions by a modified model-solid theory. The ordering parameter of the sample was determined at the same time,[34] and is listed in Table I for convenience of comparison. By correlating the weak features marked by the downward arrows in Fig. 6(a) to the corresponding PL spectrum, a slight blueshift of the minimum with respect to the PL maximum is evident, which is known as a Stokes shift.[20,41]

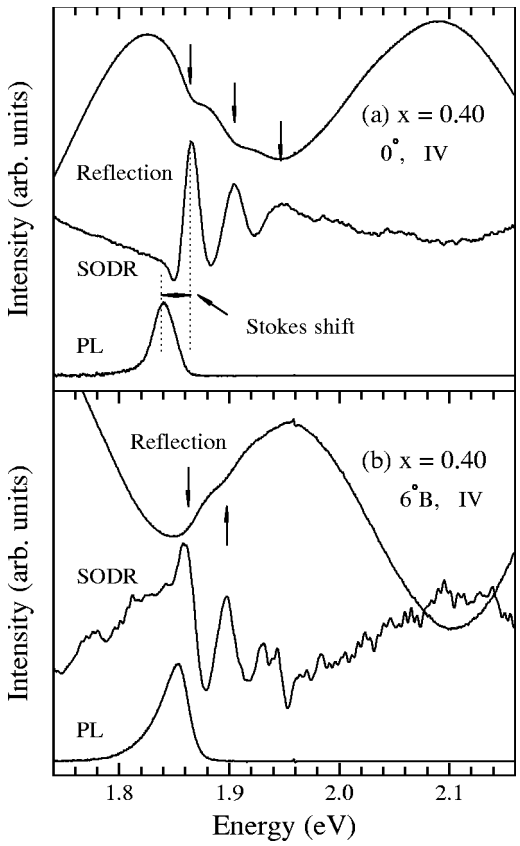

FIG. 6. Reflectivity and its second-order derivative (SODR) as well as PL spectrum of the series IV compressively strained $Ga_{0.4}In_{0.6}P/(Al_{0.66}Ga_{0.34})_{0.76}In_{0.24}P$ QW samples with (a) the 0° and (b) the $6°B$ substrates. Vertical arrows indicate the energetic positions of excitonic related transitions in the QW's.

Similar SODR line shape is observed for other samples with two exceptions. The first exception is illustrated in Fig. 6(b) for the series IV compressively strained sample with the $6°B$ substrate. On the low energy side of the first SODR maximum, no dip similar to that shown in Fig. 6(a) occurs. This suggests that no HH-like exciton state exists in this QW sample, and hence provides a further support to the bad sample-quality assumption for this sample. The second exception occurs in the two $6°A$ lattice-matched samples, where only one peak can be clearly identified in the SODR with an apparent shoulder on the high-energy side. The spectra are illustrated in Fig. 7 for the $6°A$ series I sample. For such a lattice-matched sample, the ordering is very weak.[28] The first two valence subbands are hence nearly degenerate. With an assumption of two Gaussian functions constituting the SODR peak, a good fit is obtained. The result is plotted in Fig. 7 as dashes and dash dots. The relative intensities and line widths suggest HH- and LH-like transitions[35] to the first and second fitting curves, respectively. The energetic positions, on the other hand, are consistent with the modified model-solid theory, and lead to a determination of the order-

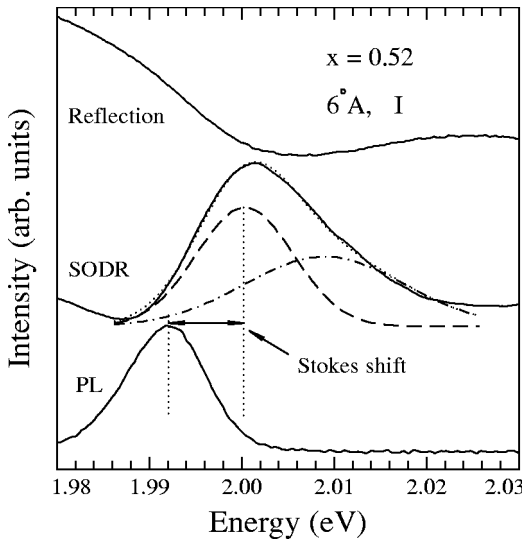

FIG. 7. Reflectivity and its SODR as well as PL spectrum of the series I lattice-matched $Ga_xIn_{1-x}P/(Al_{0.66}Ga_{0.34})_{0.52}In_{0.48}P$ QW sample with the $6°A$ substrate. The SODR peak is fitted by two Gaussian functions depicted in dashes and dash dots.

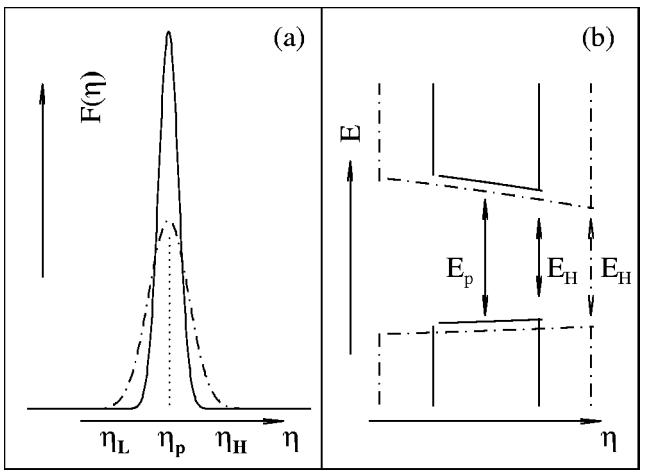

FIG. 8. Schema of (a) domain distribution function $F(\eta)$, and (b) band-edge structure due to the $F(\eta)$ in ordered QW's.

ing parameter $\eta \simeq 0.2$, which is in agreement with the common knowledge of low ordering for such a sample structure.

A detailed analysis indicates that all the strain, substrate misorientation and doping of the capping layer affect the Stokes shift of the first SODR maximum relative to the corresponding PL peak at a constant position (corresponding to a high excitation density of ~ 50 W/cm^2). (i) The compressively strained sample has a smaller Stokes shift than the lattice-matched counterpart with the same substrate and sample structure. (ii) The sample with the Zn-doped GaP capping layer has a larger Stokes shift than the sample with the same strain and substrate but undoped GaInP capping layer. (iii) The sample with the $0°$ substrate has the largest Stokes shift and the $6°A$ the smallest in the same sample series. The values of the Stokes shift are presented in Table I.

Concerning the FWHM of the first SODR peak LW_{DR}, similar dependence is only observed for the substrate misorientation that the sample with the $0°$ substrate has the largest FWHM in a same sample series. No obvious dependence can be found in the strain and doping of the capping layer. The FWHM values for most of the samples are given in Table I. By assuming a similar line shape of, e.g., Gaussian form to the first peak for all samples, a similar relation can be found among the FWHM of the first peak in their original reflectivity spectra. It is clear that the Stokes shift is smaller than the FWHM of the first peak in the reflectivity spectrum for all the single-peak samples except the bad one, if the fact is taken into account that the FWHM of the peak in the original reflectivity spectrum is about two times as large as that in the corresponding SODR spectrum.[42]

IV. DISCUSSIONS

With the experimental observations, we now check the frequently used concepts of domain distribution, band-tail states, and spatially indirect band alignment due to sequence mutations, and order-induced piezoelectric field, and try to clarify the origin of the peak narrowing as well as the saturation of the narrowing and blueshift.

A. Domain distribution?

Based on the knowledge that (i) PL transition tends to occur in small band-gap regions while reflectivity represents a spatially averaged effect[2,41] and (ii) ordered domains with different sizes correspond to different ordering parameters. Hence in characterizing the ordering not only is the ordering parameter η of particular domains needed but also the domain distribution function[4] $F(\eta)$ where $\int_0^1 F(\eta)d\eta = 1$, is necessary. A band-edge model is established as follows for the ordered GaInP/AlGaInP QW system. A Gaussian form is assumed for the function $F(\eta)$,[4] and two functions are plotted with their maximum at η_p but with different FWHM's in Fig. 8(a). The band edge is hence depicted as a function of the ordering, as illustrated in Fig. 8(b), by taking into account the order-induced band-gap reduction. The dash-dotted lines are moved slightly down to make the solid lines easy to see. η_P and E_p are, respectively, the ordering parameter and its corresponding band gap at which the domain distribution function $F(\eta)$ reaches its maximum. η_H and η_L represent the highest and lowest ordering in the same sample, respectively. Obviously, a larger linewidth of the distribution function corresponds to a larger energy difference between E_p and E_H.

The energy of the reflectivity peak is near E_p, and the FWHM of the reflectivity peak is $\sim(E_L - E_H)/2$. By assuming the linewidth of the reflectivity peak (LW_{ref}) being determined by the intrinsic linewidth δ_0 and the contribution of the domain distribution δ_η, $\delta_\eta = 2\eta\Delta\eta\Delta E_g^{\eta=1}$, we have

$$\Delta\eta = \frac{\sqrt{LW_{ref}^2 - \delta_0^2}}{2\eta\Delta E_g^{\eta=1}}, \tag{3}$$

where $\Delta\eta$ represents the FWHM of the domain distribution. LW_{ref} is about two times as large as LW_{DR}. $\Delta E_g^{\eta=1}$ is the order-induced band-gap reduction for a perfectly ordered

$Ga_xIn_{1-x}P$ and takes a value of 0.43 eV for the lattice-matched samples and 0.32 eV for the compressively strained samples.[34] With respect to the fact that (i) for large-domain partially ordered $GaInP_2$ bulk alloys, η varies only slightly[4] with $\Delta\eta \simeq 0.0048$ and (ii) the smallest FWHM of the SODR peak is 10.5 meV, δ_0 is here assumed to be 20 meV.[43] The $\Delta\eta$ can therefore be estimated for each of the samples. The results are listed in Table I. Clearly, the $\Delta\eta$ is more significant for the samples with the 0° substrate and less significant for those with the 6°*B* substrate. This is explicable with respect to the well established knowledge that for a GaInP film grown on the exact 0° substrate, two variants, i.e., $[\bar{1}11]$ and $[1\bar{1}1]$, of the CuPt-ordered structure occur, and the degree of order is not the same for the two variants.[44] For a GaInP film grown on the 6°*B* substrate, on the other hand, only a single variant CuPt-ordered structure is observed.[44–46] The doping of the GaP capping layer does not introduce systematic change to the $\Delta\eta$. Connecting to the experience of best (Al)GaInP lasers having been established from disordered material, and the 6°*B* substrate being preferable for achieving ordering,[28] it is clear that the spread of the domain distribution $F(\eta)$ plays a crucial role in the optoelectronic application. For a $\Delta\eta$ that is significantly larger than the ordered $GaInP_2$ bulk alloy, the spatial fluctuations of atomic concentration (inhomogeneities) may be the reason.[47] Relative to the bulk, even a monolayer-thick fluctuation will cause significant inhomogeneities at the interfaces for the case of a 10-nm-thick GaInP layer sandwiched in AlGaInP barriers.

With this model, the blueshift of the PL peak can be explained qualitatively in a simplified manner. At low temperature, the density of the excitation-generated electrons and holes is very low at a low excitation-power level. Most probably the carriers diffuse into the domains with extremely high ordering (η_H) and recombine there. This corresponds to low-energy emission. As these domains are limited in their occurring probability, the PL via them is weak and saturates as excitation density increases. The PL recombination will hence occur in the domains with lower ordering, leading to a shift of the total PL peak to higher energies. If the $F(\eta)$ function is sharp, the blueshift will be small. This is, in fact, the observation in the 6°*A* and 6°*B* lattice-matched samples. According to this model, the PL emission is always excitonic, which is in agreement with the measurements.

The general relation is also straightforward between the blueshift and the stable linewidth of the PL peak: a large blueshift corresponds to a wide range of domains being filled with photoinduced carriers, and hence a large stable linewidth of the PL peak. Meanwhile, at an identical excitation density, the stable PL peak energy E_{PL} is estimated to be between E_p and E_H and around the middle point. For a larger spread of $F(\eta)$ distribution the Stokes shift will take a larger value. This is also consistent with the experimental observation.

Nevertheless, with this model, it is hard to obtain a result of PL peak narrowing as the excitation-power density gets higher. It therefore suggests that there should be other reason(s) coaffecting the optical properties.

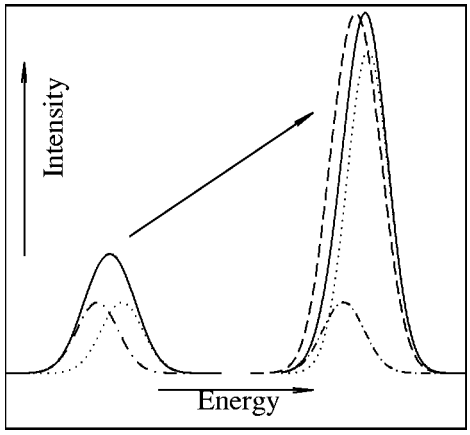

FIG. 9. Superposition of two adjacent peaks with identical intensity in the left part, and with higher energetic peak (depicted as dotted line) being four times stronger (dash-dotted) in the right part, respectively. The summation from the left part (dashed line) is scaled and moved to overlay on the right part to directly compare both the line width and the energetic position of the two summations.

B. Band-tail states or spatially indirect band alignment?

At first glance, the assumption of band-tail states seems to be able to interpret the excitation-density dependent PL transition energy. However, the assumption is questionable for two reasons in this case.

First, the narrowing is explicable only if the band-tail states are located in one or several separated energy level(s). Figure 9 schematically illustrates a two-level model. The total PL peaks are assumed to consist of a band-tail-state-related transition in dash dots with lower energy and a band-band related transition in dots with higher energy. At low excitation density, the strength of the band-tail-state-related transition is comparable to that of the band-band-related transition, the total PL peak is illustrated to the left side in Fig. 9. As the excitation density gets higher, the strength of the band-tail-state-related transition saturates quickly, due to the limited density of the states, and the total PL peak is dominated mainly by the band-band-related transition, as depicted in the right side of Fig. 9. It is apparent that the total PL peak gets narrower while shifting to higher energy as the excitation power gets higher. Note, however, that the narrowing would not be observed if the band-tail states are continuously distributed.[21]

Secondly, the assumption does not explain the similar quadratic diamagnetic shift of the PL peak at different excitation-density levels. Even if the band-tail states form excitons, the exciton effective mass and therefore the diamagnetic shift should obviously be different than that of the band-band exciton.

The model of spatially indirect recombination, originated from the assumption of either type-II band alignment in the ordered/disordered $GaInP_2$ interface[3,21–24] or sequence mutations,[26] can explain the blueshift of the PL peak as a result of the band-filling effect. However, the former assumption has been proved to be untrue that more than 10% of the order-induced band-gap reduction is due to the upward shift-

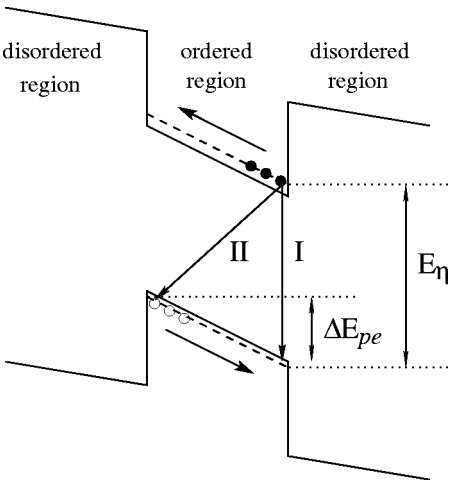

FIG. 10. Schema of the electronic band structure and the transitions within an ordered $Ga_xIn_{1-x}P$ domain possessing a piezoelectric field.

ing of the valence band.[27,34,48] For the sequence mutations, as there is a particular relation between the transition probabilities of the spatially indirect and direct transitions, increasing excitation power will simply increase the absolute intensities but not the ratio of the intensities of the two transitions. A broadening instead of narrowing is therefore predicted. Moreover, the diamagnetic shift of the spatially indirect transition should be linear with respect to the magnetic field,[49] which is contradictory to the experimental results. It is hence clear that neither the band-tail states nor the spatially indirect band alignment can serve to explain the excitation-density dependence of the PL-peak linewidth.

C. Ordering induced electric fields?

The existence of a unique [111] axis in CuPt-type ordered $GaInP_2$ alloys suggests the possibility of a piezoelectric field. This field is related to the internal electric fields for strained-layer (111) superlattices and remains even for layers of monolayer thickness.

Figure 10 illustrates the electronic band structure for an ordered domain sandwiched in disordered domains. For the QW's, this represents two types of structures. (i) In the well plane, it is an ordered domain embedding in the domains with lower ordering, and the domain size is of the order of magnitude of 100 nm or higher.[20] (ii) In the [001] direction perpendicular to the well plane, the domain is likely limited by the AlGaInP barriers and its size is about 10 nm. Due to the piezoelectric field, the optical recombination within QW's may be both direct as marked by I and ''indirect'' as marked by II for the extremal case. The energy difference between the two transitions is $\Delta E_{\mathrm{pe}} \simeq \eta^2 e_{\mathrm{pe}} S_d$, where e_{pe} is the piezoelectric field of perfect ordering and S_d is the line scale of the domains.

Under a low power excitation, the transitions occur mainly in the domains with extremely high ordering. Therefore, the FWHM of the PL peak is determined by

$$\mathrm{LW}_1 = \sqrt{\delta_0^2 + \delta_{\mathrm{pe},\perp}^2 + \delta_{\mathrm{pe},\parallel}^2}, \tag{4}$$

where δ_0 represents the intrinsic FWHM, which corresponds to the excitonic transition in an ideal QW structure free of any internal electric field and domain fluctuation. $\delta_{\mathrm{pe},\perp}$ and $\delta_{\mathrm{pe},\parallel}$ are the contributions of the piezoelectric field along the [001] direction and in the (001) well plane, respectively. They are estimated to be

$$\delta_{\mathrm{pe},\perp} \simeq \eta^2 e_{\mathrm{pe},\perp} S_{d,\perp}/2, \quad \delta_{\mathrm{pe},\parallel} \simeq \eta^2 e_{\mathrm{pe},\parallel} S_{d,\parallel}/2. \tag{5}$$

As the excitation power gets higher, more carriers are generated. This introduces two distinct effects. (i) The carriers tend to extend their region in the direction illustrated by the arrow parallel to the bottom of the conduction/valence band, and hence screen the piezoelectric field. $\delta_{\mathrm{pe},\perp}$ and $\delta_{\mathrm{pe},\parallel}$ are therefore reduced, leading to a narrowing of the PL peak. (ii) As the domain with extremely high ordering is limited in occurring possibility, the PL recombination begins to occur in domains with lower ordering, which in turn causes a broadening of the PL peak. For a high enough excitation, the contribution of $\delta_{\mathrm{pe},\perp}$ will be totally removed, and the linewidth of the PL peak will be

$$\mathrm{LW}_s = \sqrt{\delta_0^2 + \delta_{\mathrm{pe},\parallel_s}^2 + \delta_{\eta_s}^2}, \tag{6}$$

where $\delta_{\mathrm{pe},\parallel_s}$ is the residual portion of the $\delta_{\mathrm{pe},\parallel}$. δ_{η_s} is the contribution of the filled domains, $\delta_{\eta_s} \leqslant \delta_\eta$.

With the fact in mind that the linewidth tends to stabilize in a rather wide range after a particular excitation-power density ($\geqslant 40$ W/cm^2), it can be concluded that the decrease in $\delta_{\mathrm{pe},\parallel_s}^2$ is compensated by the increase in $\delta_{\eta_s}^2$, $\delta_{\mathrm{pe},\parallel_s}^2 + \delta_{\eta_s}^2 \simeq \delta_{\mathrm{pe},\parallel}^2$. The peak narrowing can hence be determined:

$$\mathrm{PN} = \mathrm{LW}_1 - \mathrm{LW}_s \simeq \frac{\delta_{\mathrm{pe},\perp}^2}{2\ \mathrm{LW}_s}, \tag{7}$$

due to $|\mathrm{LW}_1 - \mathrm{LW}_s| \ll \mathrm{LW}_s$.

The combination of Eqs. (5) and (7) gives

$$e_{\mathrm{pe},\perp} \simeq \frac{2\sqrt{2 \times \mathrm{PN} \times \mathrm{LW}_s}}{\eta^2 S_{d,\perp}}. \tag{8}$$

With this relation, we can check the order of magnitude of the order-induced piezoelectric field along the [001] direction. The results are listed in Table I of $e_{\mathrm{pe},\perp}$ and $\eta^2 e_{\mathrm{pe},\perp}$, the latter indicates the real magnitude of the field in the particular sample. They indicate the following: (i) The electric field $e_{\mathrm{pe},\perp}$ is higher for the compressively strained sample than for the lattice-matched sample with the same substrate and capping layer. This can be understood with the simple model of $Ga_{x\pm\eta/2}In_{1-x\mp\eta/2}P$ layers in ordered $GaInP_2$ such as simply strained bulklike material.[18] (ii) $e_{\mathrm{pe},\perp}$ depends on the substrate misorientation, and the 0°-substrate sample corresponds to a higher value than the 6°*B* sample in the same series. This can be understood in a similar manner. Relative to the 0° substrate, the 6°*B* substrate may result in an additional tensile while the 6°*A* substrate may result in a compressive strain to the $Ga_{x\pm\eta/2}In_{1-x\mp\eta/2}P$ ordered layers. The former reduces and the latter increases the $e_{\mathrm{pe},\perp}$. It is noted that the 6°*A* series II sample has the largest $e_{\mathrm{pe},\perp}$ value in the

same series. (iii) A general trend for $\eta^2 e_{\mathrm{pe},\perp}$ is that the sample with 0° substrate has a higher value than that with 6°*B* substrate in a same series. For the lattice-matched samples, the one with 6°*A* substrate may possesses the smallest $\eta^2 e_{\mathrm{pe},\perp}$ in the same series, due to its lowest ordering. (iv) The $e_{\mathrm{pe},\perp}$ of the samples with an undoped capping layer is much lower than the theoretical limit of 900 kV/cm,[27] and is within the experimentally observed bounds of $\leqslant$240 kV/cm in fully ordered $GaInP_2$ bulk alloy.[18] (v) The electric field $e_{\mathrm{pe},\perp}$ is obviously higher for the sample with the Zn-doped GaP capping layer than for the sample with the same substrate but undoped GaInP capping layer. In the Zn-doped GaP capping layer, there are positive net charges, which produce an additional electric field in the QW layer with the direction pointing down to the substrate, and is hence expected to enhance the intrinsic order-induced electric field. In addition, the compressive strain caused by the 410-nm-thick GaP capping layer may also cause a minor increase of the piezoelectric field.

As manifested by the model, it can interpret the narrowing of the PL peak well. For a strong enough piezoelectric field, the effect of narrowing dominates the broadening due to the scattering of domain distribution and the PL peak is expected to manifest narrowing as the excitation density increases. This is indeed the most frequent case in experiments. The only exception, however, is for the series I sample with the 6°*A* substrate, whose PL peak width shows slight broadening while the blueshift is also very small. With respect to the series II sample with the same substrate misorientation, which has a significantly enhanced internal electric field but a smaller scattering of the domain distribution, the difference can be easily understood as the change of the PL-peak width with the excitation density. For the saturation of the narrowing and blueshift of the PL peak, it is clear that at a low excitation level, the contribution to the narrowing comes from both $e_{\mathrm{pe},\perp}$ and $e_{\mathrm{pe},\parallel}$ components, and the contribution to the blueshift comes from, in addition, the effect of filling of the domains with extremely high order, whereas at a high enough excitation level, the contribution from $e_{\mathrm{pe},\perp}$ disappears. This leads to a drastically slowed down to narrowing and blueshift. For a bulk alloy, the domain linescale *S* is in both the $\parallel$ and $\perp$ directions near the domain size, and is of the order of magnitude of 100 nm or higher.[20] The saturation will hence occur only when the excitation-power density is higher than 400 W/cm^2. This explains why the blueshift of the PL peak in the bulk alloy was observable in a much wider range of excitation-power density.[21]

Meanwhile, with the effects in mind of both the scattering of domain distribution $\Delta\eta$ and the piezoelectric field causing blueshift to the PL peak, the difference in the degree of the saturation of the blueshift and narrowing for different samples is straightforward. The sample with the 0° substrate has a larger $\Delta\eta$ and higher $\eta^2 e_{\mathrm{pe},\perp}$ than the same series sample with the 6°*B* substrate. It therefore manifests a more obvious increase in the ''saturated'' region. On the other hand, the series II lattice-matched sample with the 6°*A* substrate has a narrow scattering of $\Delta\eta$, which may result in a further narrowing to the PL peak in the saturated region in the case of a strong electric field existing in the sample. A similar discussion is valid for the two compressively strained samples with the 0° substrate: the sample prepared at 750 °C possesses an identical $\Delta\eta$ but a larger $\eta^2 e_{\mathrm{pe},\perp}$, and hence still shows a slight narrowing in the saturated region.

The difference is also straightforward in the Stokes shift for different samples. At a similar level of excitation density, a larger $\Delta\eta$ results in a larger $E_p - E_{\mathrm{PL}}$, and hence a larger Stokes shift; meanwhile, a larger $\eta^2 e_{\mathrm{pe},\perp}$ corresponds to a larger residual $\Delta E_{\mathrm{pe},\parallel}$, and again a larger Stokes shift.

It is noteworthy that the model does not explain the PL from the slightly separated double-peak samples. The Stokes shift of the first SODR peak relative to the low-energy peak in the PL spectrum is significantly larger than the FWHM of the first peak in the reflectivity spectrum, indicating that the energy of the low-energy peak is even smaller than that of the transition from extremely high order domains. This rules out the possibility of relating the low-energy PL peak to (extremely high) order domains. As its origin is not clearly identified in this work, we guess it may be caused by a strain-related defect[30] occurring especially in the 6°*A* misoriented-substrate case.

V. CONCLUSION

In the excitation-density dependent PL measurements, blueshift and narrowing of the PL peak are observed in the range of up to 40 W/cm^2 and become less significant as the excitation density gets higher. They are affected by strain, substrate misorientation, and doping of the capping layer. (i) For the lattice-matched samples, the highest blueshift and peak narrowing are identified for the 0° substrate and the lowest for the 6°*A* substrate sample. For the compressive strain, the blueshift is higher for the 0° substrate than for the 6°*B* substrate sample. (ii) The peak narrowing is more significant for the lattice-matched sample than the compressively strained one, and is more significant for the sample with Zn-doped GaP capping layer than that with undoped GaInP capping layer with the same substrate and Ga composition in the QW layers. The blueshift is found to correlate directly with the stable linewidth. A larger blueshift corresponds to a larger stable linewidth of the PL peak. With the magneto-PL measurements, the PL transition is identified to be excitonic.

The optical reflectivity measurements illustrate that the Stokes shift is also affected by the strain, substrate, and doping of the capping layer. (i) The compressively strained sample has a smaller Stokes shift than the lattice-matched sample with the same substrate and sample structure. (ii) The sample with a Zn-doped GaP capping layer has a larger Stokes shift than the sample with the same substrate and the Ga composition in the QW layers but undoped GaInP capping layer. (iii) The 0° sample has the largest and the 6°*A* the smallest Stokes shift in the same sample series.

With the observations, the band-tail states and spatially indirect band alignment due to sequence mutations are concluded to be not suitable for the QW structure. A band-edge model is then established based on the concepts of domain distribution function and ordering-induced piezoelectric field, with which the experimental phenomena are well inter-

preted. The scattering of the ordering parameter $\Delta\eta$ and the piezoelectric field along [001] direction $e_{\mathrm{pe},\perp}$ are estimated. The results indicate that the $\Delta\eta$ is obviously larger than that reported in $GaInP_2$ bulk material. It plays a crucial role in optical transitions and is more significant for the samples with the 0° substrate than for the samples with the 6°*B* and 6°*A* substrates. The $e_{\mathrm{pe},\perp}$, on the other hand, is significantly lower than the theoretically predicted value and falls into the experimentally observed range for the $GaInP_2$ bulk material. The Zn-doped GaP capping layer causes an enhancement to $e_{\mathrm{pe},\perp}$.

ACKNOWLEDGMENTS

We are grateful to F. Scholz for helpful discussions and recommendations, and X. Wang for technical assistance. One of the authors (J.S.) thanks the Volkswagen-Stiftung and the Deutscher Akademischer Austauschdienst for financial support. The work was partially supported by the Shanghai Natural Science Foundation (Grant No. 02ZA14114), the National Natural Science Foundation (Grant No. 60276006) and the special funds for Major State Basic Research (Grant No. G001CB3095) of China.

*Author to whom correspondence should be addressed. Electronic address: jshao@mail.sitp.ac.cn

[1] A. Zunger and S. Mahajan, *Handbook of Semiconductors*, 2nd ed. (Elsevier, Amsterdam, 1994), Vol. 3, p. 1399, and references therein.

[2] G.S. Horner, A. Mascarenhas, S. Froyen, R.G. Alonso, K. Bertness, and J.M. Olson, Phys. Rev. B **47**, 4041 (1993).

[3] H.M. Cheong, A. Mascarenhas, S.P. Ahrenkiel, K.M. Jones, J.F. Geisz, and J.M. Olson, J. Appl. Phys. **83**, 5418 (1998).

[4] H.M. Cheong, A. Mascarenhas, J.F. Geisz, J.M. Olson, M.W. Keller, and J.R. Wendt, Phys. Rev. B **57**, R9400 (1998).

[5] S. Smith, H.M. Cheong, B.D. Fluegel, J.F. Geisz, J.M. Olson, L.L. Kazmerski, and A. Mascarenhas, Appl. Phys. Lett. **74**, 706 (1999).

[6] S.-H. Wei and A. Zunger, Phys. Rev. B **39**, 3279 (1989).

[7] S.-H. Wei and A. Zunger, Appl. Phys. Lett. **56**, 662 (1990).

[8] D.B. Laks, S.-H. Wei, and A. Zunger, Phys. Rev. Lett. **69**, 3766 (1992).

[9] S.-H. Wei, D.B. Laks, and A. Zunger, Appl. Phys. Lett. **62**, 1937 (1993).

[10] R.G. Alonso, A. Mascarenhas, G.S. Horner, K.A. Bertness, S.R. Kurtz, and J.M. Olson, Phys. Rev. B **48**, 11 833 (1993).

[11] S.-H. Wei and A. Zunger, Phys. Rev. B **49**, 14 337 (1994).

[12] F. Alsina, N. Mestres, J. Pascual, C. Geng, P. Ernst, and F. Scholz, Phys. Rev. B **53**, 12 994 (1996).

[13] S.-H. Wei and A. Zunger, Phys. Rev. B **57**, 8983 (1998).

[14] S.-H. Wei and A. Zunger, Appl. Phys. Lett. **64**, 757 (1994).

[15] J.S. Luo, J.M. Olson, S.R. Kurtz, D.J. Arent, K.A. Bertness, M.E. Raikh, and E.V. Tsiper, Phys. Rev. B **51**, 7603 (1995).

[16] P. Ernst, Y. Zhang, F.A.J.M. Driessen, A. Mascarenhas, E.D. Jones, C. Geng, F. Scholz, and H. Schweizer, J. Appl. Phys. **81**, 2814 (1997).

[17] S. Froyen and A. Zunger, Phys. Rev. B **53**, 4570 (1996).

[18] J.D. Perkins, Y. Zhang, J.F. Geisz, W.E. McMahon, J.M. Olson, and A. Mascarenhas, J. Appl. Phys. **84**, 4502 (1998).

[19] Y. Hsu, G.B. Stringfellow, C.E. Inglefield, M.C. DeLong, P.C. Taylor, J.H. Cho, and T.-Y. Seong, Appl. Phys. Lett. **73**, 3905 (1998).

[20] P. Ernst, C. Geng, G. Hahn, F. Scholz, H. Schweizer, F. Phillipp, and A. Mascarenhas, J. Appl. Phys. **79**, 2633 (1996).

[21] P. Ernst, C. Geng, F. Scholz, and H. Schweizer, Phys. Status Solidi B **193**, 213 (1996).

[22] M.C. DeLong, W.D. Ohlsen, I. Viohl, P.C. Taylor, and J.M. Olson, J. Appl. Phys. **70**, 2780 (1991).

[23] J.-R. Dong, Z.-G. Wang, X.-L. Liu, D.-C. Lu, D. Wang, and X.-H. Wang, Appl. Phys. Lett. **67**, 1573 (1995).

[24] M.J. Gregor, P.G. Blome, R.G. Ulbrich, P. Grossmann, S. Grosse, J. Feldmann, W. Stolz, E.O. Göbel, D.J. Arent, M. Bode, K.A. Bertness, and J.M. Olson, Appl. Phys. Lett. **67**, 3572 (1995).

[25] A. Sasaki, K. Tsuchida, Y. Narukawa, Y. Kawakami, Sg. Fujita, Y. Hsu, and G.B. Stringfellow, J. Appl. Phys. **89**, 343 (2001).

[26] T. Mattila, S.-H. Wei, and A. Zunger, Phys. Rev. Lett. **83**, 2010 (1999).

[27] S. Froyen, A. Zunger, and A. Mascarenhas, Appl. Phys. Lett. **68**, 2852 (1996).

[28] F. Scholz, C. Geng, M. Burkard, H.-P. Gauggel, H. Schweizer, R. Wirth, A. Moritz, and A. Hangleiter, Physica E **2**, 8 (1998).

[29] A. Moritz and A. Hangleiter, Appl. Phys. Lett. **66**, 3340 (1995).

[30] C. Geng, M. Moser, R. Winterhoff, E. Lux, J. Hommel, B. Höhing, H. Schweizer, and F. Scholz, J. Cryst. Growth **145**, 740 (1994).

[31] J. Shao, A. Dörnen, R. Winterhoff, and F. Scholz, J. Appl. Phys. **91**, 2553 (2002).

[32] E.P. O'Reilly, G. Jones, A. Ghiti, and A.R. Adams, Electron. Lett. **27**, 1417 (1991).

[33] E.P. O'Reilly and A.T. Meney, Phys. Rev. B **51**, 7566 (1995).

[34] J. Shao, A. Dörnen, R. Winterhoff, and F. Scholz, Phys. Rev. B **66**, 035109 (2002).

[35] For convenience, here the expression ''HH/LH-like'' is used just to represent the subband with heavier/lighter out-of-plane effective mass. In fact, due to the ordering induced valence-band mixing, the HH/LH notations lose their traditional meaning.

[36] J. Shao, Ph.D. thesis, Universität Stuttgart, 2002.

[37] J. Shao, D. Haase, A. Dörnen, V. Härle, and F. Scholz, J. Appl. Phys. **87**, 4303 (2000).

[38] W. Zhou, M. Dutta, D.D. Smith, J. Pamulapati, H. Shen, P. Newman, and R. Sacks, Phys. Rev. B **48**, 5256 (1993).

[39] B.V. Shanabrook, O.J. Glembocki, and W.T. Beard, Phys. Rev. B **35**, 2540 (1987).

[40] A.F. Terzis, X.C. Liu, A. Petrou, B.D. McCombe, M. Dutta, H. Shen, D.D. Smith, M.W. Cole, M. Taysing-Lara, and P.G. Newman, J. Appl. Phys. **67**, 2501 (1990).

[41] Y. Ishitani, S. Minagawa, T. Kita, T. Nishino, H. Yaguchi, and Y. Shiraki, J. Appl. Phys. **80**, 4592 (1996).

[42] G. Talsky, *Derivative Spectrophotometry* (VCH, Weinheim, Germany, 1994).

[43] The different choice of the δ_0 value, e.g., 18 meV, though less possible, will cause a significant change only to the $\Delta\eta$ of the 6°*A* lattice-matched samples. It will not affect the values of other samples obviously.

[44] D.H. Jaw, G.S. Chen, and G.B. Stringfellow, Appl. Phys. Lett. **59**, 114 (1991).

[45] L.C. Su, I.H. Ho, and G.B. Stringfellow, J. Appl. Phys. **75**, 5135 (1994).
[46] J.H. Li, J. Kulik, V. Holý, Z. Zhong, S.C. Moss, Y. Zhang, S.P. Ahrenkiel, A. Mascarenhas, and J. Bai, Phys. Rev. B **63**, 155310 (2001).
[47] E. Zolotoyabko, A. Goldner, and Y. Komem, Phys. Rev. B **60**, 11 014 (1999).
[48] T. Kippenberg, J. Krauss, J. Spieler, P. Kiesel, G.H. Döhler, R. Stubner, R. Winkler, O. Pankratov, and M. Moser, Phys. Rev. B **60**, 4446 (1999).
[49] S.H. Kwok, P.Y. Yu, J. Zeman, S. Jullian, G. Martinez, and K. Uchida, J. Appl. Phys. **84**, 2846 (1998).